



Influence of L-serine on microstructural, spectroscopic, electrical and nonlinear optical performance of ammonium dihydrogen phosphate single crystal

J. H. Joshi¹ · S. Kalainathan² · M. J. Joshi¹ · K. D. Parikh³

Received: 23 May 2019 / Accepted: 1 July 2019 / Published online: 4 July 2019
© Springer Science+Business Media, LLC, part of Springer Nature 2019

Abstract

To doubling the frequency of Nd: YAG and Nd: YLF laser sources the ammonium dihydrogen phosphate (ADP) single crystal is widely used. In the present communication, the effect of amino acid namely as L-serine on the growth and properties of ADP crystal is been reported. The slow solvent evaporation technique is adopted to grow pure and different weight percentage i.e. 0.4 wt%, 0.6 wt% and 0.8 wt% L-serine doped ADP crystals. The structural study suggested tetragonal structure symmetry of all grown crystal with single phasic nature of all of them. The amino acid dopant alters the functional group vibrations of ADP crystal as suggested in FT-IR spectroscopy. The change in morphology and presence of various elements is observed in SEM and EDAX spectroscopy. The improvement is observed in various optical properties like energy band gap, skin depth, SHG, third order nonlinear susceptibility, laser damage threshold etc. on doping the L-serine in ADP crystal. The spectra variation of refractive index of all grown crystals is studied. The pure and L-serine doped ADP crystals have posses negative kind of photoconductivity.

1 Introduction

The ammonium dihydrogen phosphate (ADP) is an excellent piezo-electric crystal utilized for variety of nonlinear optical applications [1]. It is to be known that to modify the growth rate, crystal habit etc. the impurities should be added into the crystal undertaken for study. Due to the molecular chirality and zwitter ionic structure [2] of amino acids, they are able to provide optical transparency and hardness to the materials. The Levo oriented serine consists of shorter side chain in its structure and by nature it is acts as hydrogen donor amino acid. Hence it will be easy to combine the L-serine with ADP crystal lattice.

The present authors have studied structural, spectroscopic, electrical, linear and nonlinear optical properties of pure and L-serine doped ADP crystals.

2 Experimental technique

To grow single crystals of pure and different weight percentage of L-serine doped ADP, the present authors have adopted slow solvent evaporation technique. In such technique the water is acts as a solvent. The 400 ml of water volume is taken to solute the pure ADP in it for the preparation of saturated solution. Then homogeneity of such solution is achieved by stirring the solution for 4 h using magnetic stirrer. The stirring is followed by filtration of such solution using Whatmann filter paper. The total volume of pure ADP saturated solution is subdivide into four beakers and then 0.4 gm, 0.6 gm and 0.8 gm of L-serine is added into the three glass beakers. The L-serine contained ADP solution is further stirred for another 4 h followed by filtration. All four beakers containing pure, 0.4 wt%, 0.6 wt% and 0.8 wt% L-serine doped ADP is then shield properly and the natural evaporation of water contain is taking place in dust free atmosphere. The crystals of pure and L-serine doped ADP is harvested from the each of the beakers after 20 days.

✉ J. H. Joshi
jaydeep_joshi1989@yahoo.com

✉ K. D. Parikh
ketandparikh@yahoo.co.in

¹ Department of Physics, Saurashtra University,
Rajkot 360 005, India

² School of Advanced Science, Centre of Crystal Growth, VIT
University, Vellore 632 014, India

³ Department of Physics, Shri M.P. Shah Arts & Science
College, Surendranagar 363 001, India

Figure 1 shows grown crystals. For a sake of simplicity throughout the manuscript here we adopted code as pure, 0.4 LSR, 0.6 LSR and 0.8 LSR for pure, 0.4 wt%, 0.6 wt% and 0.8 wt% L-serine doped ADP crystal.

3 Characterization techniques

The PHILIPS X'PERT MPD system is used for the powder XRD study and the obtained data is analysed using powder—X software. The THERMO NICOLET 6700 is used for FT-IR study. The wavenumber range chosen for such study is 400–4000 cm^{-1} and the potassium bromide (KBr) media is used. The SEM and EDAX spectroscopy is done using the JSM-7600F setup having voltage range from 0.1 to 30 kV and probe current range from 1 pA to ≥ 200 nA. The linear optical study i.e. UV–Vis spectroscopy is done using Shimadzu UV-2450 spectrophotometer in the wavelength of 200–900 nm. The HIOKI 3532 LCR HITERSTER is used to study the complex admittance spectroscopy for the palletized sample of crystals in the frequency rang of 10 Hz to 10 MHz and the temperature range chose is 323–373 K. Keithley 485 pm with the field variation of 5 to 100 V/cm is used to study the photoconductivity. Q-switched Nd:YAG laser of wavelength 1064 nm and input energy 0.71 J is used to study the second harmonic generation efficiency (SHG) of grown crystals. The CW He–Ne laser of wavelength 632 nm

is used to study the Z-scan. The Nd:YAG laser of 1064 nm wavelength, 10 ns pulse width and 35 cm focal length is used to study laser damage threshold of grown crystals.

4 Result and discussion

4.1 Powder XRD

Figure 2 shows the powder XRD patterns of grown crystals. The additional phase is found to be absent in case of pure and L-serine doped ADP crystal which suggested single phasic nature of grown crystals. The grown crystals have posses the tetragonal structure symmetry with slight change in unit cell parameter on doping the L-serine in ADP. Table 1 shows the unit cell parameters and unit cell volume of grown crystals.

4.1.1 Williamson–Hall analysis

To estimate the lattice stain introduced by the dopant in ADP crystal, the Williamson-Hall method is applied to the powder XRD patterns of all the grown crystals. One can calculate the limited crystallite size and the presence of crystallographic distortion or strain leading to the Lorentzian intensity distribution. The equation is expressed as follows [3]:

$$\beta \cos \theta = \frac{K\lambda}{L} + \eta \sin \theta \quad (1)$$

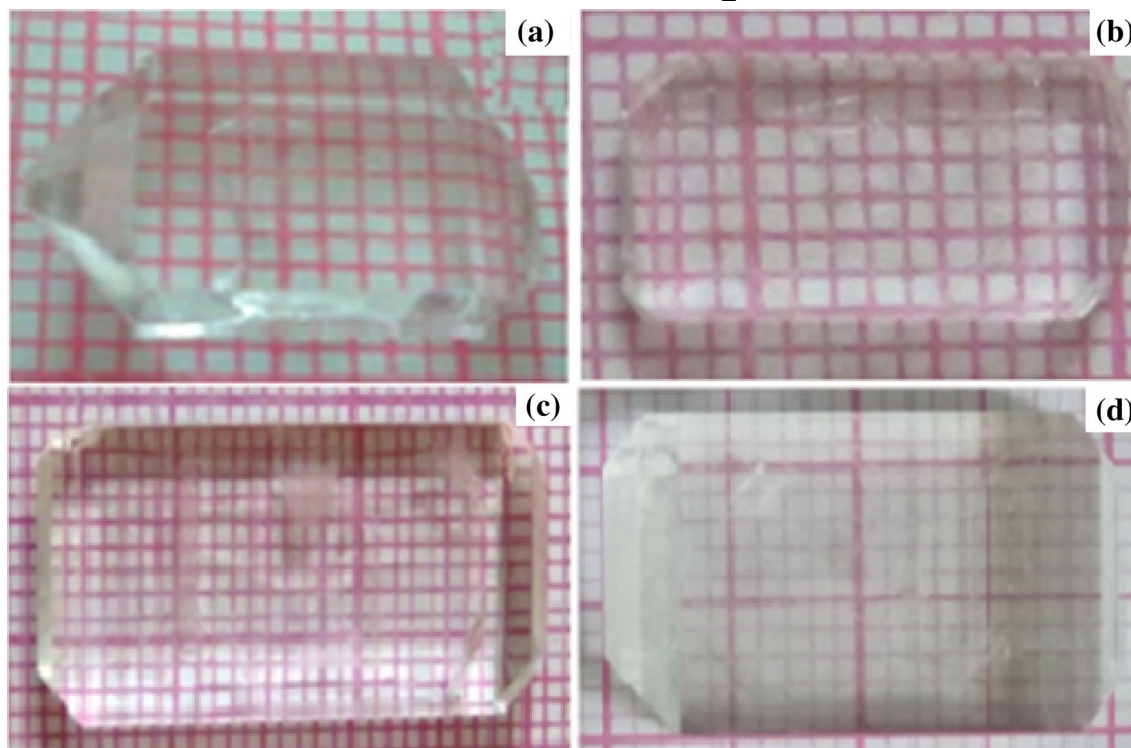


Fig. 1 Single crystal of **a** pure, **b** 0.4 wt%, **c** 0.6 wt%, **d** 0.8 wt% L-serine doped ADP

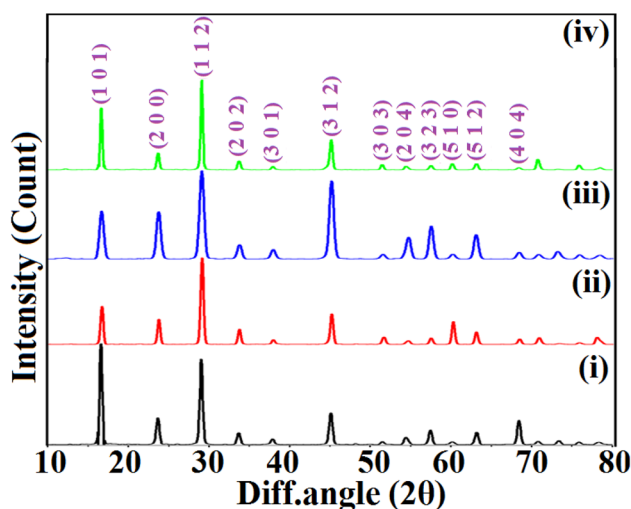


Fig. 2 Powder XRD pattern of (i) pure (ii) 0.4 wt% (iii) 0.6 wt% (iv) 0.8 wt% L-serine doped ADP crystals

Table 1 Unit cell parameters of pure and L-serine doped ADP crystals

Samples	a=b (Å)	c (Å)	Unit cell volume (Å ³)
Pure ADP	7.505	7.550	425.25
0.4 LSR	7.505	7.557	425.65
0.6 LSR	7.510	7.558	426.27
0.8 LSR	7.496	7.554	424.46

where β = full width half maximum of high intensity diffraction peaks, L = the crystallite size, η = the strain, K = constant = 0.9, λ = wavelength of incident X-rays = 1.54178 Å.

Figure 3 shows the Williamson–Hall plots of the pure and L-serine doped ADP crystals, respectively. The crystallite size and lattice strain is calculated from the intercept and slope of straight line fitting of such plots. Table 2 shows estimated values of the crystallite size and the strain of grown crystals.

From Table 2, it can be seen that on doping the different concentration of L-serine amino acid in ADP crystal the variation in crystallite size and strain is observed on major scale. For instant, among the three different concentrations of L-serine doped ADP crystals, the 0.4 wt% L-serine doped ADP crystal experiences least lattice strain and has the highest magnitude of crystallite size. Such behaviour can be understood as follows: The crystallite size corresponds to the growth of grains in single crystal. Hence, it is obvious that 0.4 wt% L-serine doped ADP crystal with highest crystallite size would possess highest grain growth at the time of crystal growth. Likewise, the microscopic grains are well conducting which ultimately

increases the conduction of material (i.e. polarization of material). Therefore, among the three different concentrations of L-serine doped ADP crystals, the 0.4 wt% L-serine doped ADP crystal has the highest magnitude of polarization which is quite beneficial to increase the nonlinear optical second harmonic generation efficiency. The forthcoming section of present communication shows the measured second harmonic generation efficiency of grown crystals.

4.2 FT-IR spectroscopy

Figure 4 shows the FT-IR spectra of pure and different weight percentage of L-serine doped ADP crystals. Such plot shows that the L-serine doping in ADP crystals alters the absorption band of pure ADP crystal that confirms the presence of L-serine in ADP. As for example, the pure ADP spectrum consists of the O–H stretching vibration of P–O–H group and N–H vibration of NH₄ group arising at 3135 cm⁻¹. The PO₄ asymmetric stretching vibration corresponds to the 1293 cm⁻¹ band. While the absorption bands for the same constituent element of ADP in the case of 0.4 wt%, 0.6 wt% and 0.8 wt% L-serine doped ADP are changed slightly. As for example, peaks at 2872 cm⁻¹ and 2868 cm⁻¹ for 0.4 wt%, 0.6 wt% and 0.8 wt% L-serine doped ADP crystals correspond to the C–H stretching vibration. Likewise, the C=O stretching of COOH of L-serine arises at 1716 cm⁻¹, 1718 cm⁻¹ and 1720 cm⁻¹ for 0.4 wt%, 0.6 wt% and 0.8 wt% L-serine doped ADP, respectively. The band assignments of different constituents of pure and L-serine doped ADP crystals are tabulated in Table 3.

4.3 SEM study

Figure 5 shows the SEM images of pure and L-serine doped ADP crystals. From the figure, it can be seen that for the pure and 0.4 wt% L-serine doped ADP crystals, the crystallites are aggregated at one common point of the lattice as bunched hillocks, while for the 0.6 wt% and 0.8 wt% L-serine doped ADP crystals, the crystallites remain distinguishable. Hence, the change in morphology on doping the L-serine in ADP confirms the presence of dopant in ADP crystal.

4.4 EDAX spectroscopy

Figure 6 shows the EDAX spectra of grown crystals. Further, from Table 4, it can be seen that the percentage of carbon is increased as the doping amount of L-serine is increased in ADP crystal, which again indicates the successful doping of L-serine in ADP crystal.

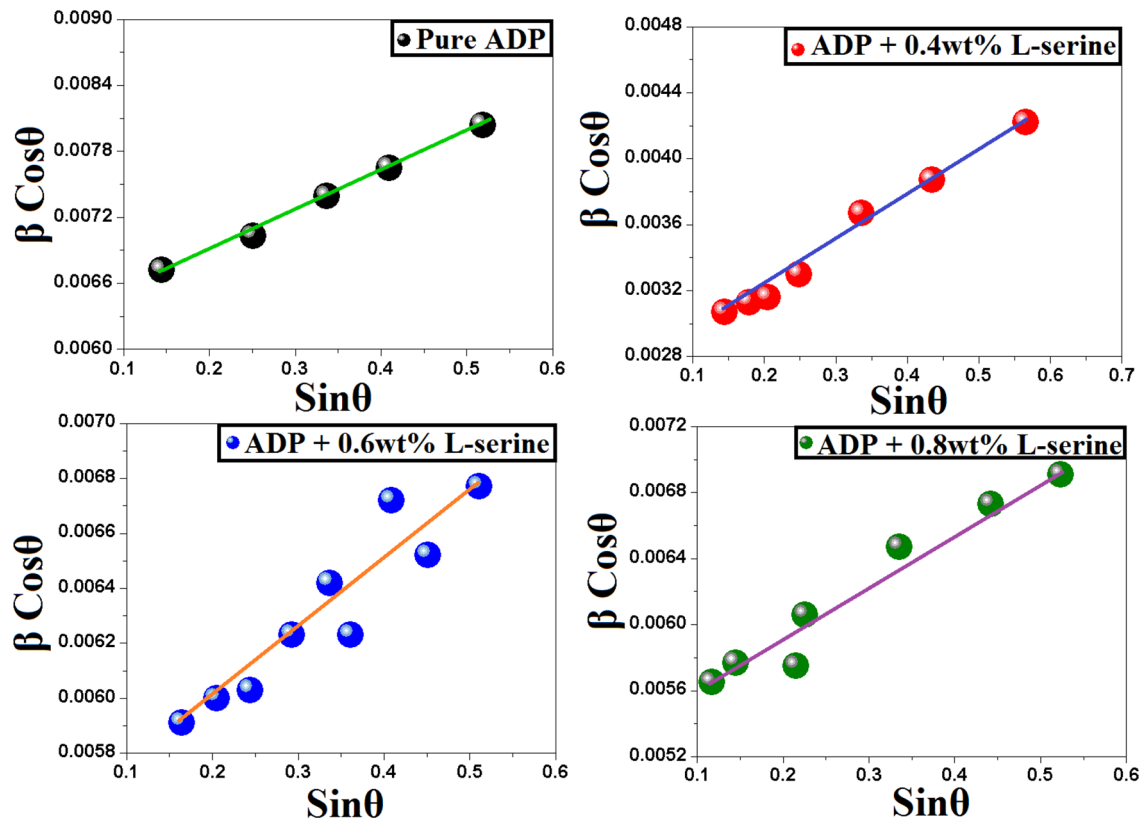


Fig. 3 Williamson–Hall plots of grown crystals

Table 2 The Williamson–Hall plot parameters

Sample	Crystallite size (L) (μm)	Strain (η) (mm)
Pure ADP	0.190	0.166
0.4 LSR	0.361	0.077
0.6 LSR	0.224	0.267
0.8 LSR	0.235	0.328

4.5 UV–Visible spectroscopy

Figure 7 shows UV–Vis transmittance spectra of pure and different weight percentage L-serine doped ADP crystals. The optical transmittance is increase as the wavelength and doping concentration of L-serine is increase in ADP crystals. The pure ADP crystal shows 67% maximum transmittance in entire visible range while the doped ADP crystals shows 90% (0.4 LSR), 93% (0.6 LSR) and 98% (0.8 LSR) maximum transmittance. Hence, as mentioned earlier, due to molecular chirality and zwitter ionic structure of L-serine the optical transmittance is improved. The same results are obtained in case of L-alanine doped ADP crystals [4].

Moreover, here we have studied the other optical parameters for pure and L-serine doped ADP crystals like optical

energy band gap, refractive index, skin depth, refractive index dispersion below the energy band gap etc. the equations used to determine such parameters is given elsewhere [5].

Figure 8 shows optical energy band gap of pure and L-serine doped ADP crystals. The energy band is deduced by taking the extrapolation over X-axis of such plot. The obtained value of such parameter for all grown crystals is mentioned in respective plots. Here one can see that the optical energy band is enhanced on doping the L-serine in ADP, hence the doped crystals finds variety of applications in the field of optoelectronics [6]. It is desirable for nonlinear optical crystals that such crystals should posses the large energy band because the energy band gap is the measure of polarization for any dielectric material.

Figure 9 shows spectra variation of refractive index of pure and L-serine doped ADP crystals. From figure one can see that the trend of refractive index over wavelength range is exactly opposite than that of transmittance for all grown crystals. Hence the L-serine doped ADP crystal with less refractive index compare to pure ADP can be utilize for antireflection proposes.

Figure 10 shows the skin depth of pure and L-serine doped ADP crystal over a energy region undertaken. As

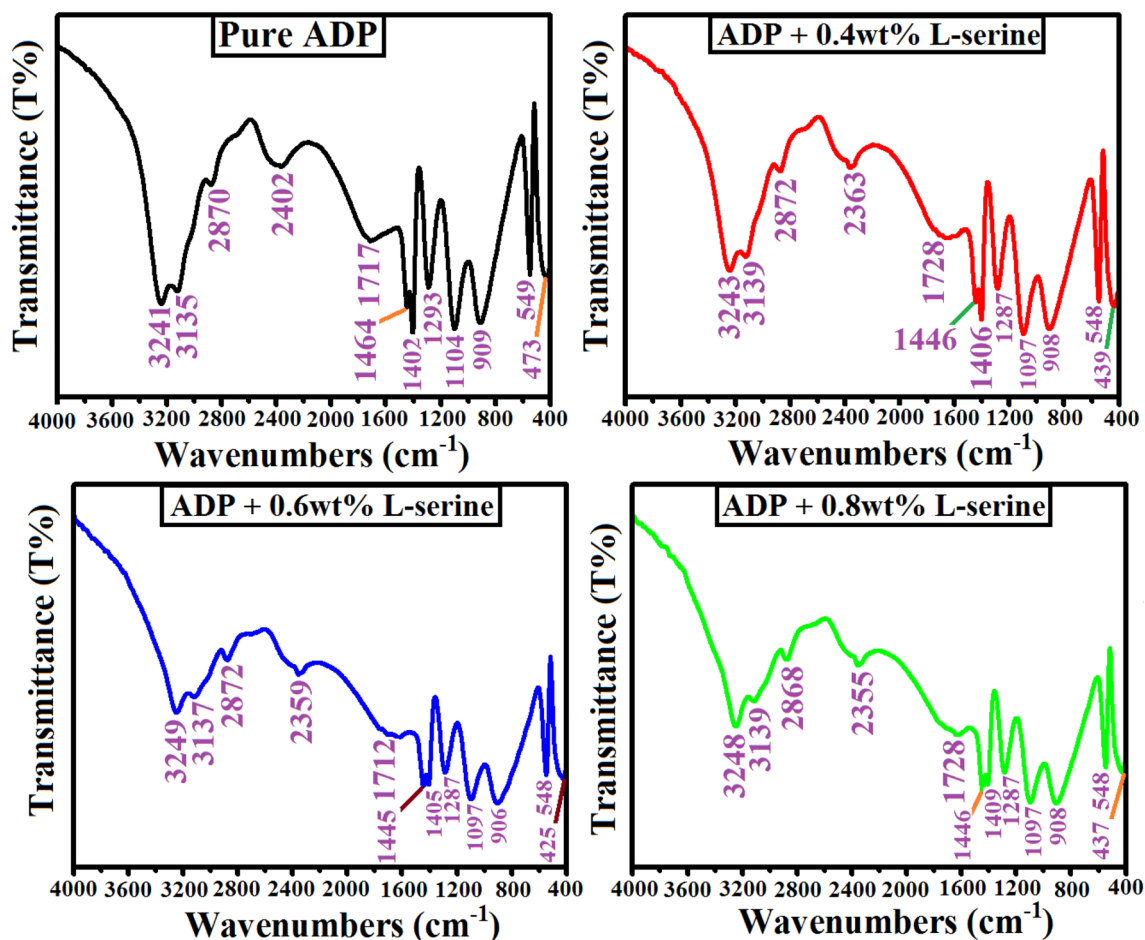


Fig. 4 FT-IR spectra of pure and L-serine doped ADP crystals

Table 3 Band assignments of pure and L-serine doped ADP crystals

Wavenumbers (cm ⁻¹)				Band assignment
Pure ADP	0.4 LSR	0.6 LSR	0.8 LSR	
3135	3243	3249	3245	O–H vibration of P–O–H group and N–H vibration of NH ₄
3135	3139	3137	3139	
2870	2872	2872	2868	Symmetric stretching of C–H of L-serine doped ADP
2402	2362	2357	2355	Hydrogen Bond
1717	1716	1718	1720	O–H bending, C=O stretching of COOH
1464	1445	1445	1445	N–H vibration, C–O stretching
1402	1406	1405	1409	Bending vibration of ammonia
1293	1287	1287	1287	Combination of asymmetric stretching of PO ₄ with lattice
1104	1097	1097	1098	P–O–H stretching, C–O stretching
909	907	906	908	P–O–H stretching, C–H stretching
549	548	548	548	PO ₄ vibration
473	439	425	437	

per the definition the skin depth is the amount of electromagnetic radiation penetrate inside the crystal, the skin depth is more for L-serine doped ADP crystals compare to pure ADP crystal. Moreover the peak value of skin

depth is mentioned in respective plot, hence from the such value it can be notice that the skin depth peak is shifting toward the high energy region as the doping concentration of L-serine is increased in ADP crystal. Therefore, it is

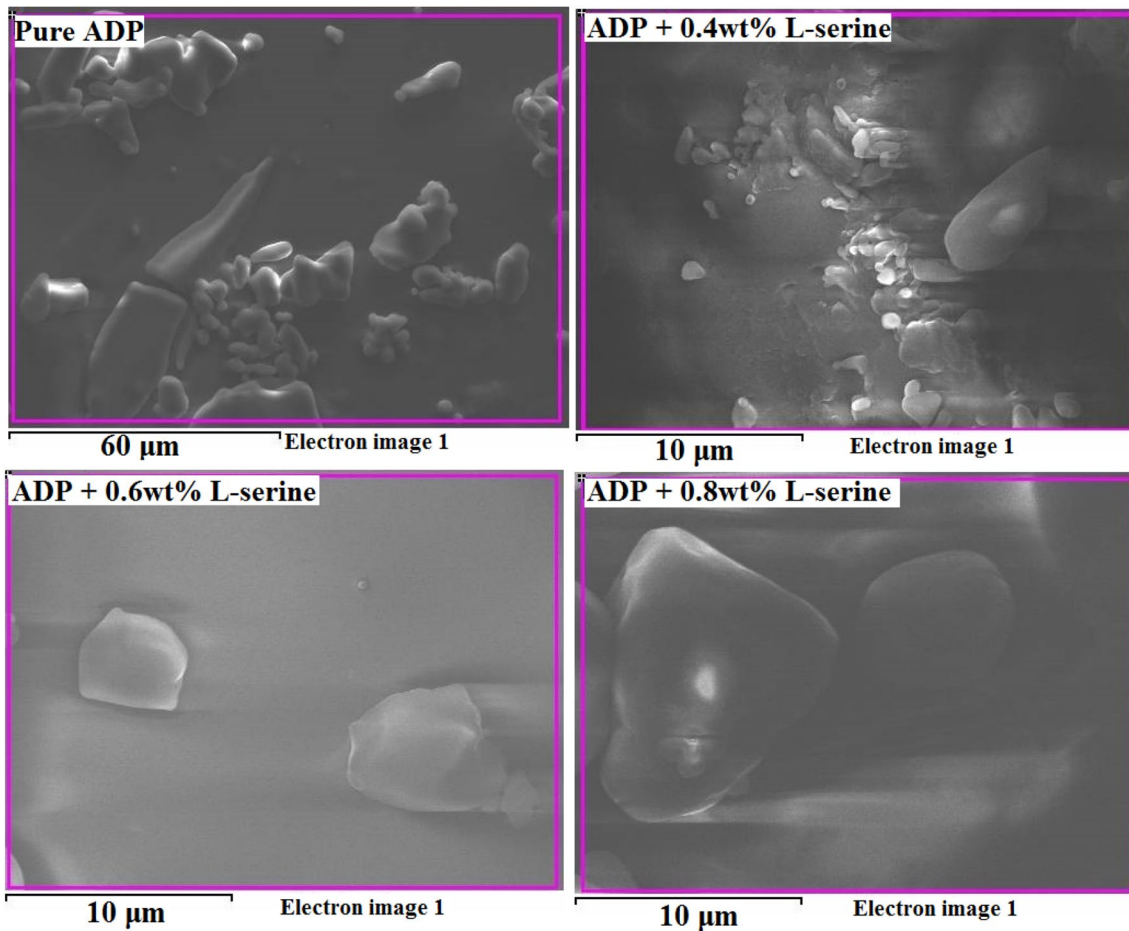


Fig. 5 SEM images of grown crystals

worthy to mention the skin depth as a consequence of the optical transmittance.

4.6 Refractive index dispersion below the energy band gap

To study the refractive index dispersion below the energy band gap for pure and L-serine doped ADP crystals, here we consider the Wemple–DiDomenico Single oscillator model [7]. Such model consist of inter band transition of electron as an single oscillator.

Figure 11 shows the refractive index dispersion below the energy band gap for pure and L-serine doped ADP crystals. By fitting the such data in straight line manner, here we have calculated the single oscillator energy (E_0), the dispersion energy (E_d) and the momentum of such oscillator model (M_{-1} and M_{-3}). The calculated values of them is tabulated in Table 5.

From Table 5 it is found that the single oscillator energy (E_0) is decrease on doping the L-serine in ADP crystal. It is desire for such parameter to be as low as possible because

it is corresponds to the average bond strength of given material. Hence on doping the L-serine in ADP the bond strength of ADP will reduced as reflect in decrement in E_0 . Therefore the incorporation of L-serine in ADP crystals can be expected by mean of lowering the single oscillator energy. Moreover, the E_0 parameter for 0.4 wt% L-serine doped ADP crystal is least among the other concentrations, hence that crystal posses superior nonlinear optical quality.

4.7 Photoconductivity

Figure 12a–d shows the variation of dark and photo current versus applied field plot for all grown crystals. The dark current is found to be greater than photo current due to the negative photoconductivity [8]. Such behaviour is attributed to the reduction of charge carrier and their life time in the presence of radiation. The negative photoconductivity of grown crystals is useful for the UV and IR detector applications [9].

Fig. 6 EDAX spectrum of **a** pure ADP, **b** 0.4 wt%, **c** 0.6 wt%, **d** 0.8 wt% L-serine doped ADP crystals

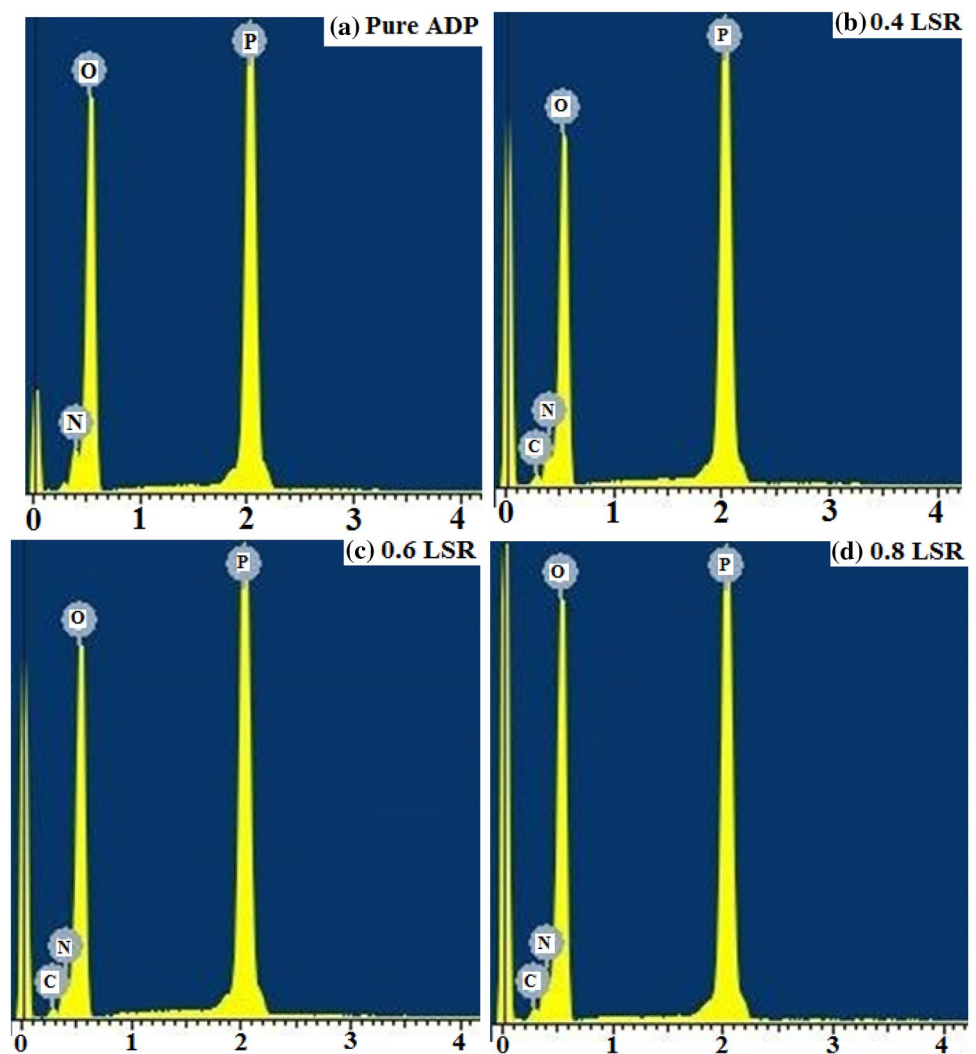


Table 4 EDAX analysis of pure and L-serine doped ADP crystals

Sample	Carbon (C)		Nitrogen (N)		Oxygen (O)		Phosphorous (P)	
	wt%	at.%	wt%	at.%	wt%	at.%	wt%	at.%
Pure ADP	–	–	10.54	13.46	64.48	72.11	24.98	14.43
0.4 LSR	5.91	8.88	9.21	11.88	54.43	61.47	30.45	17.77
0.6 LSR	6.23	9.34	8.57	10.42	54.43	61.56	30.67	18.68
0.8 LSR	7.43	11.23	7.56	9.43	55.23	62.41	29.78	16.93

4.8 Complex admittance spectroscopy

The complex admittance spectroscopy is useful to the interlayer formation at electro–electrolyte interface and the charge carrier motion. Such spectroscopy consists of capacitance and conductance simultaneously as a function of temperature or frequency. The equation used for both parameters is given elsewhere [10].

Figure 13 shows temperature variation of capacitance at angular frequency 100 rad s^{-1} for pure and L-serine doped ADP crystals. The formation of interlayer at

electrode–electrolyte interface and thermally activated charge carrier motion leads to increase the capacitance of grown crystals as the temperature is increased. By comparing the magnitude of capacitance, it is found that the 0.4 wt% L-serine doped ADP crystal have posses highest magnitude among the other concentrations. Such behaviour corresponds to fact that the material with highest polarizability should posses the highest magnitude of capacitance. Moreover, as per the Clausius–Massotti relation [11], the material with higher capacitance as well as higher polarizability would posses higher second harmonic generation efficiency. The

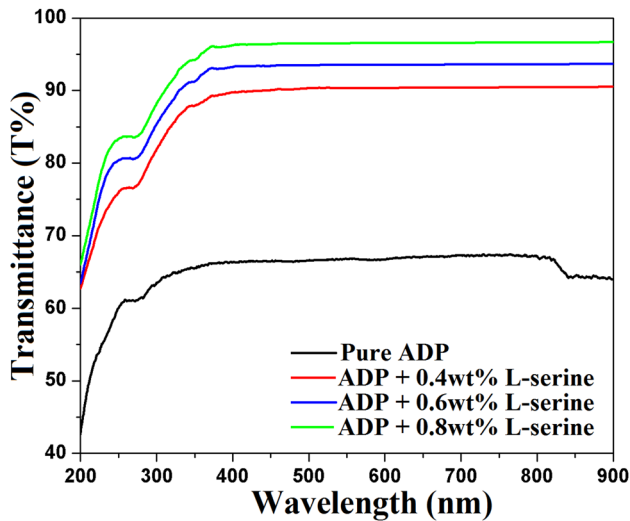


Fig. 7 Transmittance spectra of pure and L-serine doped ADP crystals

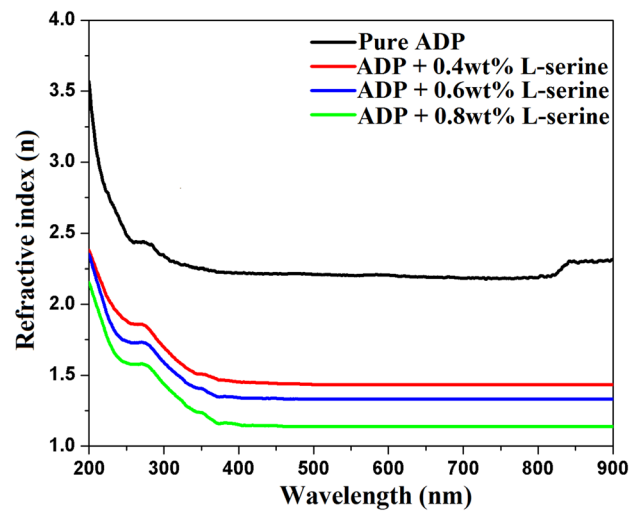


Fig. 9 Refractive index plot of pure and L-serine doped ADP crystals

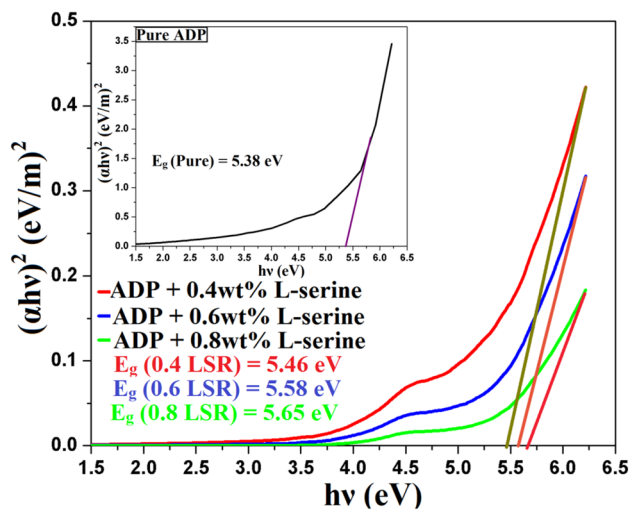


Fig. 8 Optical energy band gap plots for pure and L-serine doped ADP crystals

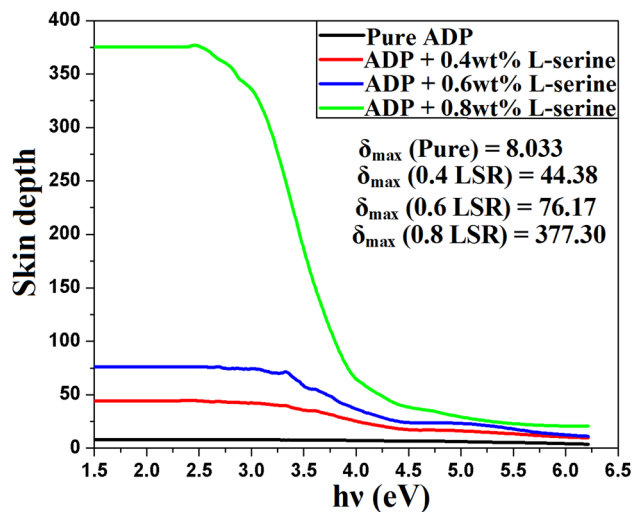


Fig. 10 Skin depth of pure and L-serine doped ADP crystal

second harmonic generation efficiency of pure and L-serine doped ADP crystals is discussed in forthcoming section.

Figure 14 shows the temperature variation of the conductance for pure and L-serine doped ADP crystals at angular frequency 100 rad s^{-1} . Alike, the capacitance the conductance is increased with the temperature which suggest the thermally activated process occurs within grown crystals. Also, the magnitude of conductance is found to be high in the case of L-serine doped ADP crystals compare to pure ADP crystals. Among the three different doping concentration of L-serine in ADP crystal, the 0.4 wt% L-serine doped ADP crystal has posses the highest magnitude of conductance. Such behaviour corresponds to the fact that the dopant causes the defect in terms of vacancy created in hydrogen

bonding. Such defect leads to enhance the conductance of grown crystals.

4.9 Second harmonic generation efficiency (SHG)

The nonlinear optical SHG efficiency of pure and different weight percentage L-serine doped ADP crystals is measured using the Kurtz and Parry powder NLO technique. For such experiment the output energy of pure KDP, pure ADP and different weight percentage L-serine doped ADP crystals is measured. By taking the ratio of output energy of different crystals over output energy of pure KDP and pure ADP, the SHG efficiency is determined. The SHG efficiency of pure and L-serine doped ADP crystals is listed in Table 6.

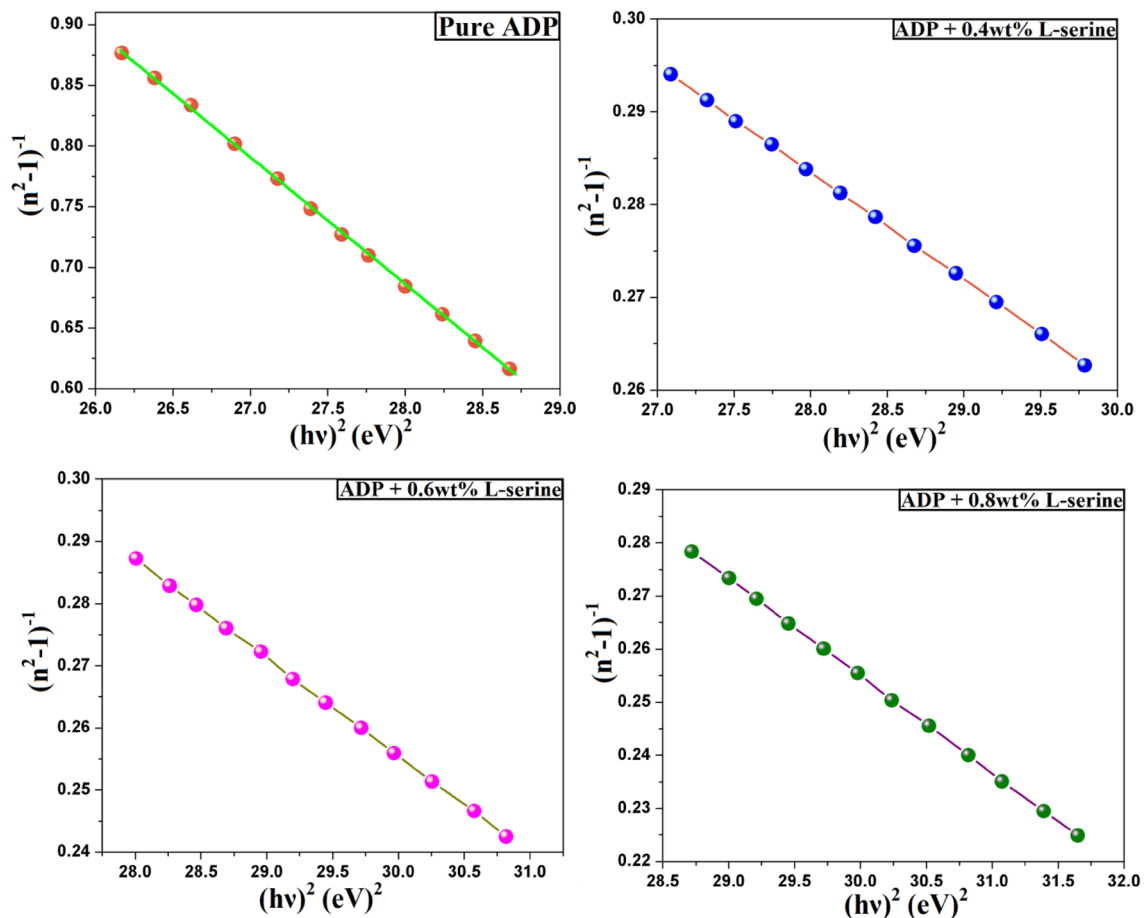


Fig. 11 Refractive index dispersion plots of pure and L-serine doped ADP crystals

Table 5 Dispersive parameters of pure and L-serine doped ADP crystals

Sample	E_d (eV)	E_0 (eV)	M_{-1}	M_{-3}
Pure ADP	1.63	5.58	0.27681	0.00801
0.4 LSR	3.46	2.09	1.64957	0.37527
0.6 LSR	3.05	2.23	1.36909	0.27595
0.8 LSR	2.87	2.31	1.24173	0.23275

From the above table, one can notice that the SHG efficiency of ADP crystal is increased on doping the L-serine in it. The same results are obtained in L-arginine doped KDP crystals [12].

Amino acids consist of a proton donating carboxy ($-\text{COOH}$) group and the proton accepting amino (NH_3^+) group. Among which the carboxy group and protonic bonds are responsible for the SHG efficiency enhancement of the parent material.

Figure 15 shows the side chain of the L-serine molecule. The L-serine possess short side chain of hydroxy group link with carboxy group, i.e. $-\text{CH}_2(\text{OH})$, due to which it is easy

to remove hydrogen from the side chain of L-serine and hence the L-serine often acts as a proton donor. During the course of L-serine doping in ADP, the proton and carboxy groups are introduced in structure of ADP, which ultimately increases the SHG efficiency of ADP crystal.

Further, such an increase in SHG efficiency of ADP crystal on doping the L-serine can be attributed to the phonon induced structure displacements, which results the large electronic polarizability and ultimately the large SHG efficiency of grown crystals.

Moreover, one can estimate the SHG efficiency of grown crystals based on the Miller rule, The Miller rule states that the second harmonic generation efficiency of any nonlinear optical crystals can be written as a sum of linear susceptibilities. The crystals that will exhibit large nonlinear effects are those with a large linear susceptibility at the relevant frequencies of the effect considered and as per the well-known relation $P = \epsilon_0 \chi E$, where P = polarization and χ = linear susceptibility, i.e. the polarization is directly proportional to the linear susceptibility, hence the crystal with higher polarizability would acquire a higher susceptibility and ultimately a higher second harmonic generation efficiency [11].

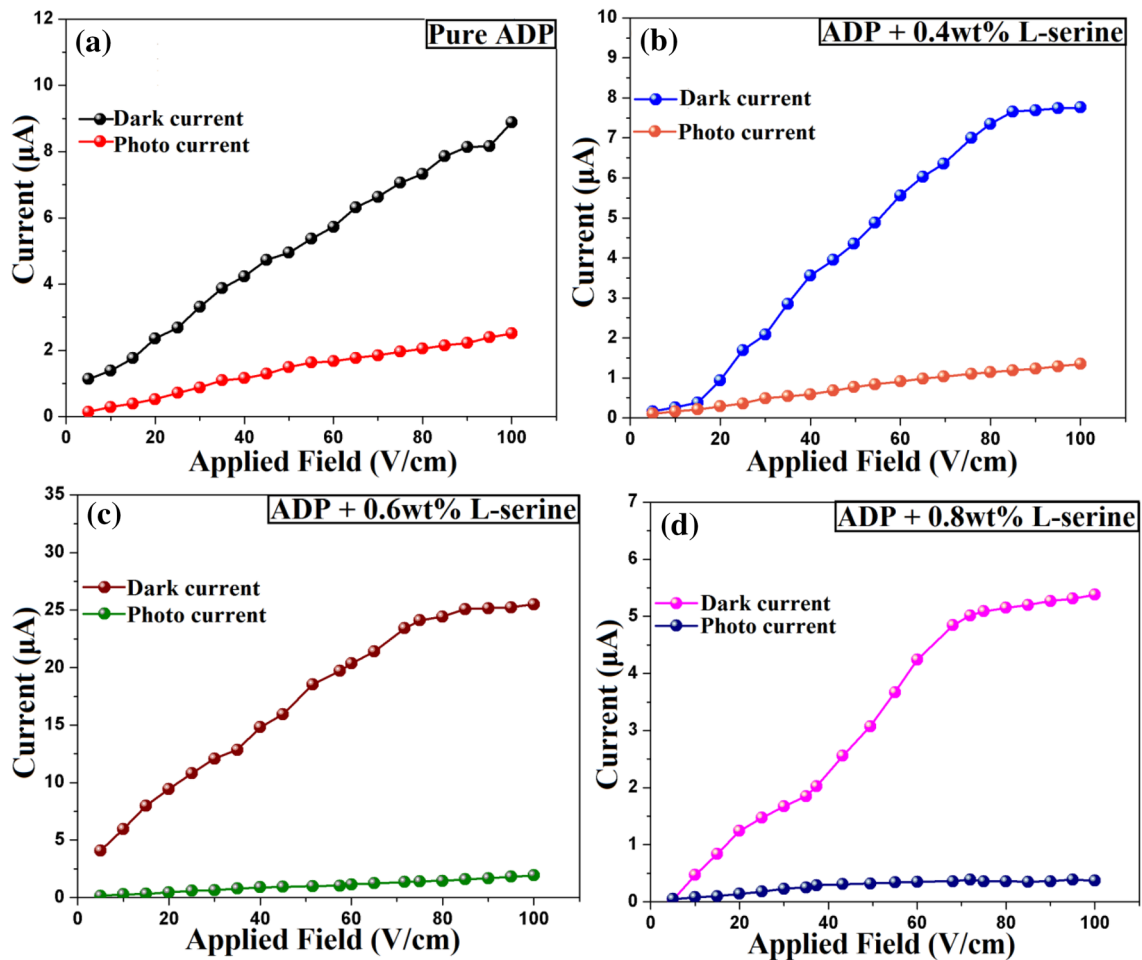


Fig. 12 Photoconductivity plots of pure and L-serine doped ADP crystals

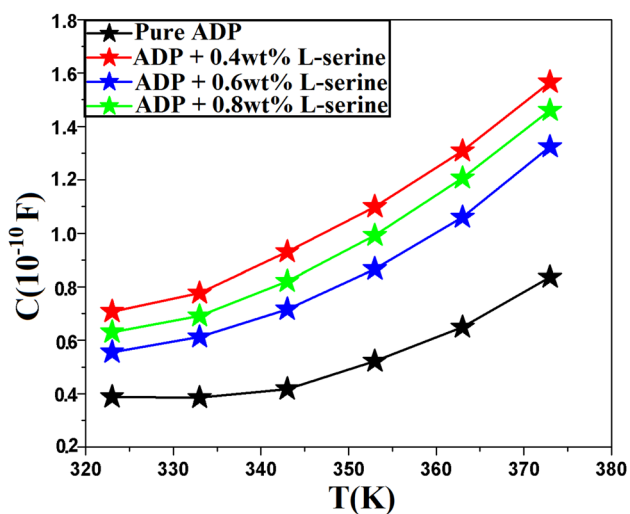


Fig. 13 Capacitance plots of pure and L-serine doped ADP crystals at $\omega = 100 \text{ rad s}^{-1}$

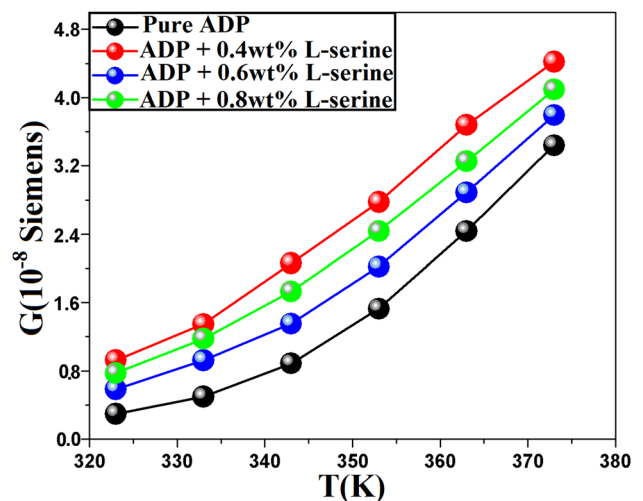
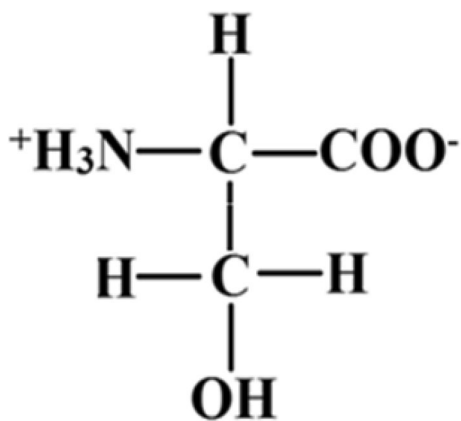


Fig. 14 Conductance plot of pure and L-serine doped ADP crystals at $\omega = 100 \text{ rad s}^{-1}$

Table 6 SHG efficiency of pure and L-serine doped ADP crystals

Sample	Output energy (mJ)	SHG efficiency	
		W.R.T. pure KDP	W.R.T. pure ADP
Pure KDP	19.5	1	–
Pure ADP	40.3	2.06	1
0.4 LSR	47.8	2.39	1.18
0.6 LSR	44.3	2.22	1.10
0.8 LSR	46.4	2.34	1.15

**Fig. 15** Side chain of L-serine molecule

4.10 Third harmonic nonlinear optical susceptibility (Z-scan)

On the subsequence of improvement observed in SHG efficiency of grown crystals, we are tempted to determine the magnitude and sign of third order nonlinear optical parameters for our grown crystals such as nonlinear optical absorption coefficient, nonlinear optical refractive index and nonlinear optical third order susceptibility using the Z-scan experiment. Previously, many authors have used the Z-scan technique for the determination of nonlinear optical third order susceptibility and related parameters for variety of materials [13–15]. The equations used for the calculation of different parameters in Z-scan are given elsewhere [5].

Presently, the Z-scan experiment is done in open and close aperture manner for all the grown crystals. Figure 16a–d is the Z-scan spectra of pure and different weight percentage L-serine doped ADP crystals in open and close aperture manner. On analysing the close aperture plots it is found that, such plots of pure, 0.4 wt% and 0.6 wt% L-serine doped ADP exhibits the self focusing phenomena as those plots shows valley followed by peak nature. Likewise, the same plot for 0.8 wt% L-serine doped ADP crystals consist of self defocusing phenomena as that plot shows peak

followed by valley nature. Hence the grown crystals, they can be utilizing for different nonlinear optical applications [16–18].

Now on observing the open aperture plots of pure and 0.6 wt% L-serine doped ADP crystal, it is found that the normalized transmittance of both crystals is decreases gradually due to the reverse saturable absorption phenomena. While the same plot for 0.4 wt% and 0.8 wt% L-serine doped ADP crystals shows gradual increment in normalized transmittance suggested presence of saturable absorption phenomena.

The various third order nonlinear optical parameters such as difference of peak and valley, nonlinear optical refractive index, nonlinear optical absorption coefficient and nonlinear optical third order susceptibility of pure and L-serine doped ADP crystals are tabulated in Table 7.

On comparing the results of Z-scan from Table 5, it can be observed that the L-serine amino acid improves the third order nonlinear optical susceptibility of ADP crystal. Further, due to higher molecular polarizability and higher delocalization of π -electron cloud [19], the 0.4 wt% L-serine doped ADP crystal posses highest magnitude of $\chi^{(3)}$. Such result is in accordance with SHG efficiency of that crystal.

4.11 Laser damage threshold (LDT)

For the laser damage threshold study of grown crystals, here we have measured power density [5]. The obtained powder density of pure and L-serine doped ADP crystals are mentioned in Table 8.

For a nonlinear optical crystal, it is desired to have large threshold against the intense laser radiation. The crystal with crystalline perfection, higher molecular chirality and ability of polarization may have higher LDT. From Table 6, such characteristic may attributed to the 0.4 wt% L-serine doped ADP crystal among the other concentration.

5 Conclusion

The successful growth of pure and different weight percentage of L-serine doped ADP crystals is made. The crystals with single phase and tetragonal structure are been grown. The presence and alteration of various functional groups of ADP crystals on account of L-serine observed from FT-IR spectroscopy. The presence of various elements and the change in morphology of pure and L-serine doped ADP crystal is confirmed by EDAX and SEM study. The L-serine doping in ADP crystals is found to beneficial in terms of improvement in optical transmittance, energy band gap, second and third order nonlinear optical efficiency and the threshold against the laser.

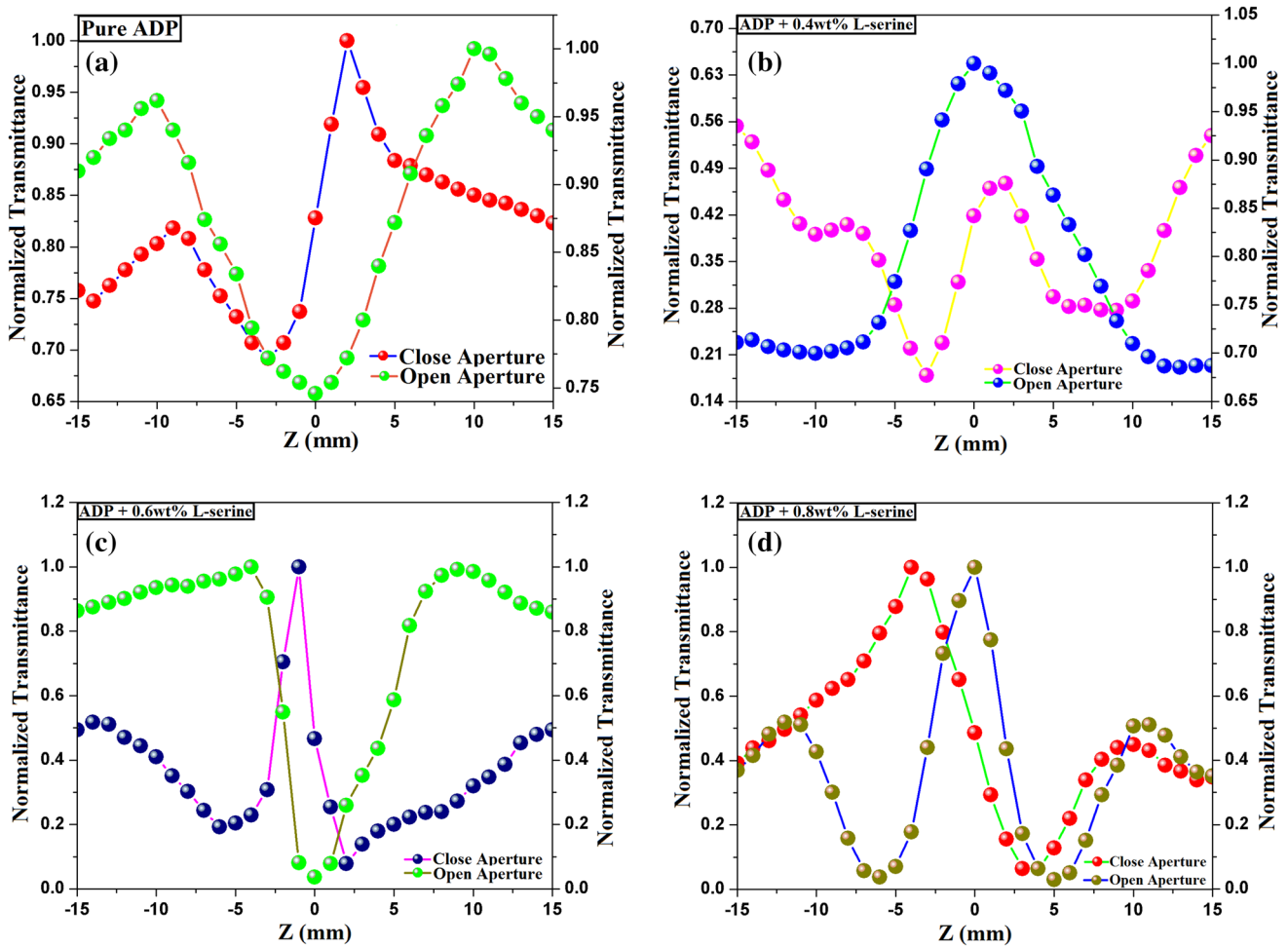


Fig. 16 Z-scan spectra of a pure ADP, b 0.4 wt%, c 0.6 wt%, d 0.8 wt% L-serine doped ADP crystals

Table 7 Z-scan parameters of pure and L-serine doped ADP crystals

Sample	ΔT_{p-v}	n_2 (cm ² /W)	β (cm/W)	$\chi^{(3)}$ (esu)
Pure ADP	0.00196	6.34×10^{-11}	9.55×10^{-6}	1.73939×10^{-5}
0.4 LSR	0.00619	7.02×10^{-10}	3.09×10^{-5}	6.13674×10^{-5}
0.6 LSR	0.00635	6.46×10^{-10}	1.52×10^{-6}	4.84375×10^{-6}
0.8 LSR	0.00596	7.05×10^{-9}	1.40×10^{-6}	5.03257×10^{-5}

Table 8 Power density values of pure and L-serine doped ADP crystals

Sample	Power density (P_d) (GW/cm ²)
Pure ADP	3.55
0.4 LSR	14.7
0.6 LSR	9.30
0.8 LSR	9.75

Acknowledgements The authors are thankful to UGC, New Delhi, for funding under DRS-SAP and DST, New Delhi, for FIST. The authors also acknowledge the encouragement and keen interest of Prof. H.H.Joshi, Head, Department of Physics, Saurashtra University, Rajkot. One of author (JHJ) is highly thankful to Mr. S.G.Khandelwal, Deputy Director, Forensic Science Laboratory, Ahmadabad for allowing him to carry out such research activity.

Author contributions JHJ: has grown the single crystals, characterizes them, analysed the data and write the manuscript, communicated papers to the said journal. SK: provided research facility such as Z-scan and Laser Threshold Damage. MJJ: given valuable suggestions, done fruitful discussion and provided constructive comments on said manuscript. KDP: has suggested research topic, supervise the research work and act as a corresponding author jointly with J.H.Joshi.

Data availability The authors of present communication confirm that the data will be available on request.

References

1. D.N. Nikogasyan, *Nonlinear Optical Crystals: A Complete Survey* (Springer, Heidelberg, 2005)
2. K.D. Parikh, D.J. Dave, B.B. Parekh, M.J. Joshi, Thermal, FT-IR and SHG efficiency studies of L-arginine doped KDP crystals. *Bull. Mater. Sci.* **30**, 105–112 (2007)
3. J.H. Joshi, D.K. Kanchan, M.J. Joshi, H.O. Jethva, K.D. Parikh, Dielectric relaxation, complex impedance and modulus spectroscopic studies of mix phase rod like cobalt sulfide nanoparticles. *Mater. Res. Bull.* **93**, 63–73 (2017)
4. F. Akhtar, J. Podder, Structural, optical, electrical and thermal characterization of pure and L-alanine doped ammonium dihydrogen phosphate crystals. *J. Cryst. Proc. Technol.* **1**, 18–25 (2011)
5. J.H. Joshi, S. Kalainathan, D.K. Kanchan, M.J. Joshi, K.D. Parikh, Effect of L-threonine on growth and properties of ammonium dihydrogen phosphate crystal. *Arab. J. Chem.* **2**, 2 (2017). <https://doi.org/10.1016/j.arabjc.2017.12.005>
6. M. Parthasarathy, M. Ananthraja, R. Gopalkrishnan, Growth and characterization of large single crystal of L-serine methyl ester hydrochloride. *J. Cryst. Grow.* **340**, 118–123 (2012)
7. S.H. Wemple, M. Jr, DiDomenico, behaviour of electronic dielectric constant in covalent and ionic materials. *Phys. Rev. B* **3**(4), 1338–1350 (1971)
8. R.H. Bube, *Photoconductivity of Solids* (Wiley, New York, 1981)
9. V.N. Joshi, *Photoconductivity* (Marcel Dekker, New York, 1990)
10. R. Ertugrul, A. Tataroglu, Influence of temperature and frequency on dielectric permittivity and ac conductivity of Au/SnO₂/n-Si (MOS) structures. *Chin. Phys. Lett.* **29**, 077304 (2012)
11. J.H. Joshi, G.M. Joshi, M.J. Joshi, H.O. Jethva, K.D. Parikh, Complex impedance, FT-Raman and photoluminescence spectroscopic studies of pure and L-phenylalanine doped ammonium dihydrogen phosphate single crystals: the correlation with hydrogen bonding defect. *Ionics* (2019). <https://doi.org/10.1007/s11581-018-2834-6>
12. K.D. Parikh, D.J. Dave, B.B. Parekh, M.J. Joshi, *Bull. Mater. Sci.* **30**(2), 105–112 (2007)
13. S. Zongo, M.S. Dhlamini, A.P. Kerasidou, P. Beukes, B. Sahraoui, M. Maaza, Linear and nonlinear optical absorption characterization of natural laccaic acid dye. *Appl. Phys. B* **120**(3), 389–396 (2015)
14. A. Diallo, S. Zongo, P. Mithunzi, S. Rehman, S.Y. Alqaraawi, W. Soboyejo, M. Maaza, Z-scan and optical limiting properties of Hibiscus Sabdariffa dye. *Appl. Phys. B* **117**(3), 861–867 (2014)
15. S. Zongo, K. Sanusi, J. Britton, P. Mthunzi, T. Nyokong, M. Maaza, B. Sahraoui, Nonlinear optical properties of natural laccaic acid dye studied using Z-scan technique. *Opt. Mater.* **46**, 270–275 (2015)
16. R. Ashok Kumar, R. Ezhil Vizhi, N. Vijayan, G. Bhagavannarayanan, D. Rajan Babu, Growth, crystalline perfection and Z-scan studies of nonlinear optical alpha-lithium iodate single crystal. *J. Pure Appl. Ind. Phys.* **1**(1), 61–67 (2010)
17. V. Natarajan, T. Sivanesan, S. Pandi, Third order non-linear optical properties of potassium aluminium sulphate single crystals by Z-scan technique. *Ind. J. Sci. Technol.* **3**, 656–658 (2010)
18. P.V. Dhanaraj, N.P. Rajesh, Investigations on crystal growth, structural, optical, dielectric, mechanical and thermal properties of a novel optical crystal: nicotinium nitrate monohydrate. *J. Cryst. Growth* **318**, 974–978 (2011)
19. J.H. Joshi, K.P. Dixit, K.D. Parikh, H.O. Jethva, D.K. Kanchan, S. Kalainathan, M.J. Joshi, Effect of Sr²⁺ on growth and properties of ammonium dihydrogen phosphate single crystal. *J. Mater. Sci. Mater. Electr.* **29**, 5837–5852 (2018)

Publisher's Note Springer Nature remains neutral with regard to jurisdictional claims in published maps and institutional affiliations.